Journal of Colloid and Interface Science 585 (2021) 178–183

Contents lists available at ScienceDirect

Journal of Colloid and Interface Science

journal homepage: www.elsevier.com/locate/jcis

Short Communication

# Tail unsaturation tailors the thermodynamics and rheology of a self-assembled sugar-based surfactant

Johan Larsson[a], Anna E. Leung[b], Christian Lang[c], Baohu Wu[c], Marie Wahlgren[d], Tommy Nylander[a,e], Stefan Ulvenlund[d,f], Adrian Sanchez-Fernandez[d,*]

[a] Physical Chemistry, Department of Chemistry, Box 124, 221 00 Lund, Sweden
[b] European Spallation Source, Box 176, 221 00 Lund, Sweden
[c] Jülich Centre for Neutron Science (JCNS) at Heinz Maier-Leibnitz Zentrum (MLZ), Forschungszentrum Jülich GmbH, Lichtenbergstr. 1, 85748 Garching, Germany
[d] Food Technology, Engineering and Nutrition, Box 124, 221 00 Lund, Sweden
[e] NanoLund, Lund University, Box 124, 221 00 Lund, Sweden
[f] EnzaBiotech AB, Scheelevägen 22, 22363 Lund, Sweden

## GRAPHICAL ABSTRACT

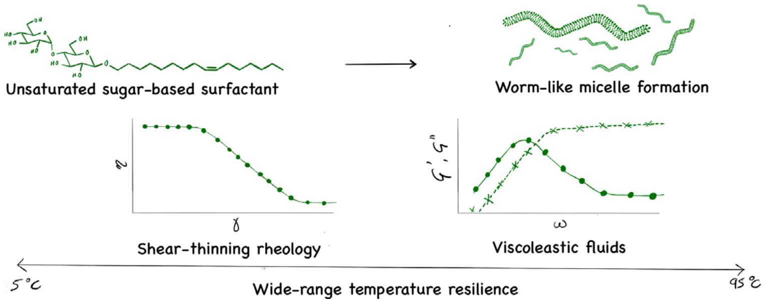

## ARTICLE INFO

*Article history:*
Received 22 October 2020
Revised 16 November 2020
Accepted 17 November 2020
Available online 21 November 2020

*Keywords:*
Unsaturated surfactant
Sugar-based surfactant
Worm-like micelle
Viscoelastic fluid
Small-angle scattering

## ABSTRACT

*Hypothesis:* The self-assembly of long-tail surfactants results in the formation of nanoscale structures, e.g. worm-like micelles, with the ability to modify the rheology of the system. However, micelle formation, and thus the alteration of the rheology, is subject to the high Krafft temperature of saturated long-tail surfactants. Hexadecylmaltosides are sustainable surfactants that, in solution, form tailorable viscoelastic fluids. The preparation of monounsaturated sugar-based surfactants is hypothesised to reduce the Krafft point compared to the saturated analogues, therefore increasing the temperature range where the surfactant remains in the micellar form.

*Experiments:* Here we report the synthesis and characterisation of a novel sugar-based surfactant with an unsaturated C16-tail, namely palmitoleyl-β-D-maltoside ($\beta\text{-}C_{16\text{-}1}G_2$). Differential scanning calorimetry was used to probe the temperature stability of the system. The rheology of $\beta\text{-}C_{16\text{-}1}G_2$ solutions was investigated by means of rotational and oscillatory rheology, and these results were connected to the mesoscopic structure of the system as shown by small-angle neutron and X-ray scattering, and dynamic light scattering.

*Findings:* The presence of a double bond on the alkyl chain moiety leads to a depression in the Krafft point, allowing the surfactant to form a thermodynamically stable micellar solution over a wide range

---

* Corresponding author.
*E-mail address:* adrian.sanchez-fernandez@food.lth.se (A. Sanchez-Fernandez).

https://doi.org/10.1016/j.jcis.2020.11.063

of temperatures, i.e. 5–95 °C. The surfactant self-assembles into worm-like micelles which, upon entanglement in the semi-dilute regime, result in the formation of a non-Newtonian, viscoelastic fluid. These observations have important implications in the development of new sustainable formulated products, enabling the preparation of surfactant phases with remarkable thermal resilience.

## 1. Introduction

The morphology of surfactant self-assemblies can be described in terms of the monomer packing, expressed as the so-called critical packing parameter, which in turn gives the preferred curvature of the surfactant at the interface with the solvent [1]. Apart from the common morphologies for the micelles (e.g. spherical, ellipsoidal, and cylindrical), surfactants can self-assemble into very long semiflexible aggregates, called worm-like micelles (WLM) [2]. The most studied group of WLM-forming surfactants are ionic surfactants in salt solutions, where the electrostatic repulsion between the headgroups of the surfactants is screened by the salt, decreasing the average micelle curvature [3,4]. High concentrations of surfactants in these solutions result in entangled networks of WLM. These systems show viscoelasticity, which is important for several applications, e.g. modification of the rheological properties of formulated products [5,6].

The surfactants prone to forming the most elongated micelles and, thus, the most viscous aqueous solutions are those with long alkyl chains (≥16). However, those surfactants also show the lowest solubility and the highest Krafft points, which limits their use in technological applications at room temperature [7]. Amphiphilic molecules with a double bond in the alkyl chain show higher solubility in water and lower Krafft points compared to the saturated analogues [8]. The inclusion of a chain unsaturation thus allows for the self-assembly of long-tail surfactants (e.g. up to 22 carbons) into micellar structures over a wider temperature range. Raghavan et al. reported the behaviour of monounsaturated $C_{22}$ cationic surfactants with very low Krafft points (<0 °C) [9]. The change in the rheological behaviour, associated with the formation of entangled WLM, was induced by the addition of salts and the viscoelasticity was retained up to high temperatures (90 °C). The synthesis and self-assembly of unsaturated $C_{18}$ betaines were studied by Kelleppan et al., showing that a monounsaturated tail leads to a reduction of the Krafft point from 50 °C for the saturated surfactant analogue to below 2.5 °C for the unsaturated surfactant [10]. This allowed the system to form WLM at room temperature and display non-Newtonian behaviour. Moore et al. have studied long-chain unsaturated surfactants with sugar units as the headgroup and a polyethylene glycol linker between the headgroup and tail [11,12]. The Krafft point was observed to be lower when the alkyl tail contained a double bond compared to a saturated chain. This allowed surfactants with up to $C_{22}$ tails to remain soluble at room temperature and to form viscous WLM solutions.

Since society is striving towards using more environmentally friendly products, it is important to find surfactants that can be manufactured from renewable raw materials. Indeed, sugar-based surfactants can be produced by sustainable means and have rich self-assembly behaviour [13]. The self-assembly behaviour and rheological properties of hexadecylmaltosides in aqueous solutions have recently been shown to strongly depend on the anomeric configuration of the surfactant [14,15]. In particular, it was shown that the equatorial configuration of the headgroup (β) leads to the formation of WLM with remarkable viscoelastic properties [15]. However, these surfactants were found to have a Krafft point above room temperature, thus limiting their possible technological applicability. Here, for the first time, the synthesis and characterisation of an unsaturated-tail sugar-based surfactant, palmitoleyl-β-D-maltoside (β-$C_{16\text{-}1}G_2$), is presented. The characteristic transition temperatures, rheological behaviour and micelle structure for this surfactant in aqueous solution were studied and compared to the saturated analogue, hexadecyl-β-D-maltoside (β-$C_{16}G_2$).

## 2. Results and discussion

Fig. 1a shows the molecular structure of the synthesised surfactant palmitoleyl-β-D-maltoside. Details of the synthesis and NMR spectroscopic data are included in the ESI. The temperature at which an aqueous solution of 50 mM β-$C_{16\text{-}1}G_2$ dissolves was characterised using differential scanning calorimetry (DSC) and compared to the same concentration of the saturated analogue, β-$C_{16}G_2$. Fig. 1b presents the DSC thermogram of 50 mM β-$C_{16\text{-}1}G_2$ and 50 mM β-$C_{16}G_2$ between 5 and 95 °C.

The DSC results do not show any change in heat capacity, Cp, between 95 °C and 5 °C for 50 mM of the unsaturated β-$C_{16\text{-}1}G_2$, while a peak for the saturated β-$C_{16}G_2$ is observed around 27 °C. This peak is associated with the dissolution enthalpy of the saturated surfactant at this concentration. No peak was observed for β-$C_{16\text{-}1}G_2$, as this surfactant remains dissolved even after storing the surfactant solution at 4 °C for several weeks. This behaviour was visually confirmed for all the different β-$C_{16\text{-}1}G_2$ concentrations prepared during this study, i.e. from 1 mM to 100 mM. These results confirm that one of the key features of the tail unsaturation, i.e. the lowering of the Krafft point relative to the saturated analogue, applies to sugar-based surfactants in the same way as has

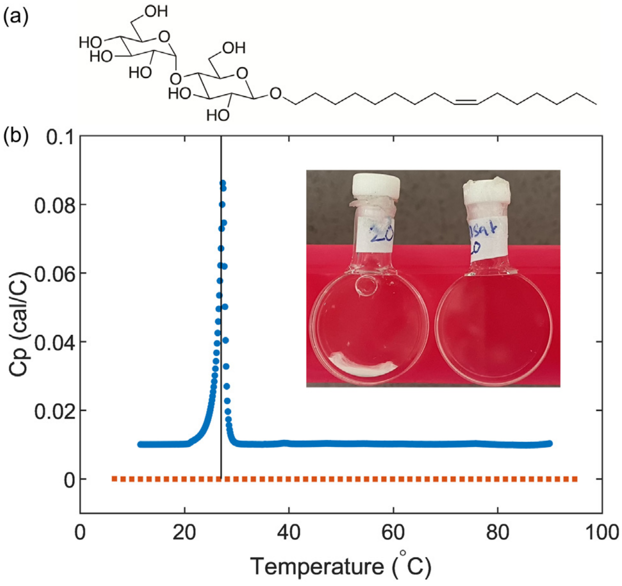

**Fig. 1.** (a) Molecular structure of β-$C_{16\text{-}1}G_2$ and (b) DSC thermogram of 50 mM β-$C_{16\text{-}1}G_2$ (■) and 50 mM β-$C_{16}G_2$ (●). The black vertical line marks the Krafft temperature of β-$C_{16}G_2$ at 27 °C. Inset: Photograph of aqueous solutions of 20 mM β-$C_{16}G_2$ (left) and 20 mM β-$C_{16\text{-}1}G_2$ (right) after 72 h stored at room temperature.

been previously reported for ionic [9], zwitterionic [10], and ethoxylated non-ionic surfactants [11].

One of the macroscopic fingerprints of WLM formation is the non-Newtonian character of the fluid. The behaviour of a 100 mM β-C$_{16\text{-}1}$G$_2$ solution at 25 °C was therefore probed using linear and oscillatory rheology. In addition, the tensile strength of a 100 mM β-C$_{16\text{-}1}$G$_2$ sample was characterised using tensile strength texture analysis at 25 °C and these results were compared with those from a 100 mM β-C$_{16}$G$_2$ sample. The results from the rheological and mechanical characterisation of the surfactant solutions are shown in Fig. 2.

The flow curve shows that the system is a viscous, non-Newtonian shear thinning liquid with a zero-shear viscosity of 150 Pas (Fig. 2a). At increasing shear, the micelles align in the direction of the flow, decreasing the number of entanglement points and thus also the viscosity. The reproducible jump in viscosity at shear rates of 0.2–0.3 s$^{-1}$ indicates the presence of a yield point. We hypothesise that this change in the viscosity might indicate a regime with thixotropic behaviour, but further investigation is required to elucidate the origin of this. The oscillatory rheology results (Fig. 2b) display a viscoelastic behaviour, where the viscous modulus (G″) is dominant at low frequencies and the elastic modulus (G′) is dominant at high frequencies. The relaxation time (τ) can be calculated from the inverse of the angular frequency (ω) where G′ = G″ (i.e. 13.5 Pa), yielding τ = 5 s. The Maxwellian model (see ESI) fits relatively well to the data (Fig. 2c). This strongly indicates that the system can be described using a single relaxation time as the network relaxation is dominated by micelle breakage rather than reptation [16]. The small deviation of G′ at high frequencies reveals that the system is not perfectly Maxwellian. There is also a deviation from the model for G″ at high frequencies. This is a common deviation for WLM systems and is attributed to the presence of fast relaxation modes that are not accounted for in the Maxwell model (e.g. stretching and cross-sectional fluctuations) [17].

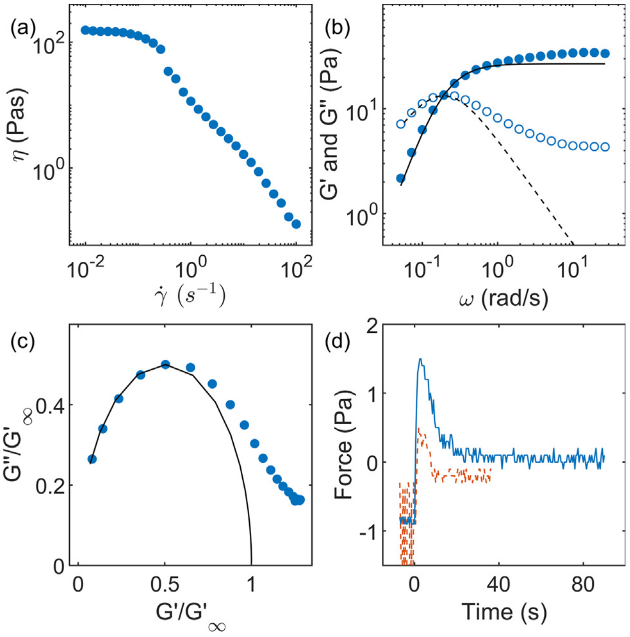

**Fig. 2.** Rheological and mechanical properties of an aqueous solution of 100 mM β-C$_{16\text{-}1}$G$_2$ at 25 °C. (a) Viscosity as a function of shear rate. (b) Oscillatory shear frequency sweep results and fits for a strain of 10%: Elastic modulus G′ (●), viscous modulus G″ (○). The solid and dashed lines are the Maxwell model fit of G′ and G″, respectively. (c) Normalized Cole-Cole plot with the black line showing the Maxwell fit. (d) Tensile strength texture analysis of 100 mM of the unsaturated β-C$_{16\text{-}1}$G$_2$ at 25 °C (blue solid line) and 100 mM of the saturated β-C$_{16}$G$_2$ at 50 °C (red dashed line).

The rheological properties of β-C$_{16\text{-}1}$G$_2$ resemble that of β-C$_{16}$G$_2$ in the sense that it is both shear-thinning and viscoelastic [15]. The zero-shear viscosity is slightly higher for β-C$_{16\text{-}1}$G$_2$ than for β-C$_{16}$G$_2$ (86 Pas), but upon shearing the viscosity becomes very similar for both surfactants. The yield point is also seen for both systems, but at higher concentrations for β-C$_{16}$G$_2$ (200 mM) [15]. Interestingly, the viscoelastic properties of β-C$_{16\text{-}1}$G$_2$ are better described with the Maxwell model than those of β-C$_{16}$G$_2$. This is most evident at high frequencies, where G″ displays a more distinct decrease and G′ is closer to reaching a plateau for β-C$_{16\text{-}1}$G$_2$ than β-C$_{16}$G$_2$ [15]. As the relaxation time of both systems is similar, the origin of this difference could be attributed to the micelle internal dynamics (e.g. β-C$_{16\text{-}1}$G$_2$ break faster than the β-C$_{16}$G$_2$) [18]. The rheological properties of five unsaturated non-ionic surfactants that form viscoelastic WLM solutions at room temperature were reported by Moore et al. [12]. Two of these, referred to as Glc-EO4-C22:1 and Gal-EO3-C18:1 in the original report, have a longer relaxation time (*ca.* 200 and 25 s respectively) than β-C$_{16\text{-}1}$G$_2$, even at lower concentrations (19.2 and 25.6 mM). An explanation for the remarkable rheological behaviour of these surfactants can be attributed to their long alkyl tail (C$_{22}$ and C$_{18}$), which promotes the formation of more elongated and entangled WLM than those reported here.

Despite the close similarities observed by the linear and oscillatory rheology measurements of the two systems compared here, an obvious difference in properties is that on visual inspection the unsaturated surfactant solutions appear to have a notably more “stringy” flow behavioud than the saturated counterpart. To quantify this difference, tensile strength texture analysis was employed. In this method, the force required to lift a probe from a sample solution is measured as a function of the distance travelled. The data reveal that a significantly larger force is required to lift the probe from the 100 mM β-C$_{16\text{-}1}$G$_2$ solution compared to the 100 mM β-C$_{16}$G$_2$ solution (Fig. 2d). Furthermore, the β-C$_{16\text{-}1}$G$_2$ solution sticks to the probe, resulting in the formation of a liquid column even when the probe is several centimetres above the surface of the solution, see Fig. S11. This behaviour is not seen for β-C$_{16}$G$_2$ where the contact between the sample and the probe is lost immediately when the probe is lifted above the surface of the solution. It is noteworthy that this stark difference in behaviour is not captured in the other rheological properties of the system and that it cannot be correlated to the current structural models of the micelles in the dilute regime. However, it may be hypothesised that the “slimy” and “stringy” character of the unsaturated surfactant solutions could be attributed to the formation of transient micellar structures induced by the extensional flow [19].

The non-Newtonian character of sugar-based surfactant solutions has been previously attributed to the formation and entanglement of WLM [15,20]. In order to probe the origin of the non-Newtonian behaviour for the unsaturated surfactant, the structure of β-C$_{16\text{-}1}$G$_2$ micelles was determined using small-angle neutron scattering (SANS), small-angle X-ray scattering (SAXS) and dynamic light scattering (DLS). SANS and SAXS data, together with the DLS results, are presented in Fig. 3.

At 10 mM surfactant concentration, the system is expected to be in the dilute regime, as previously reported for the saturated analogue [15]. Under these conditions, the structure of the micelles could be extracted with no need to account for intermicellar interactions. The results from the structural characterisation of the β-C$_{16\text{-}1}$G$_2$ micelles reveal the formation of WLM with an average contour length of 9200 ± 600 Å and a persistence length of the rigid domains of the micelle of 215 ± 5 Å. The size of the micelle cross-section was found to be 15.1 ± 0.2 Å for the radius of the hydrophobic core and 14.5 ± 0.3 Å for the thickness of the solvated headgroup layer. DLS results show that the micelle structure is

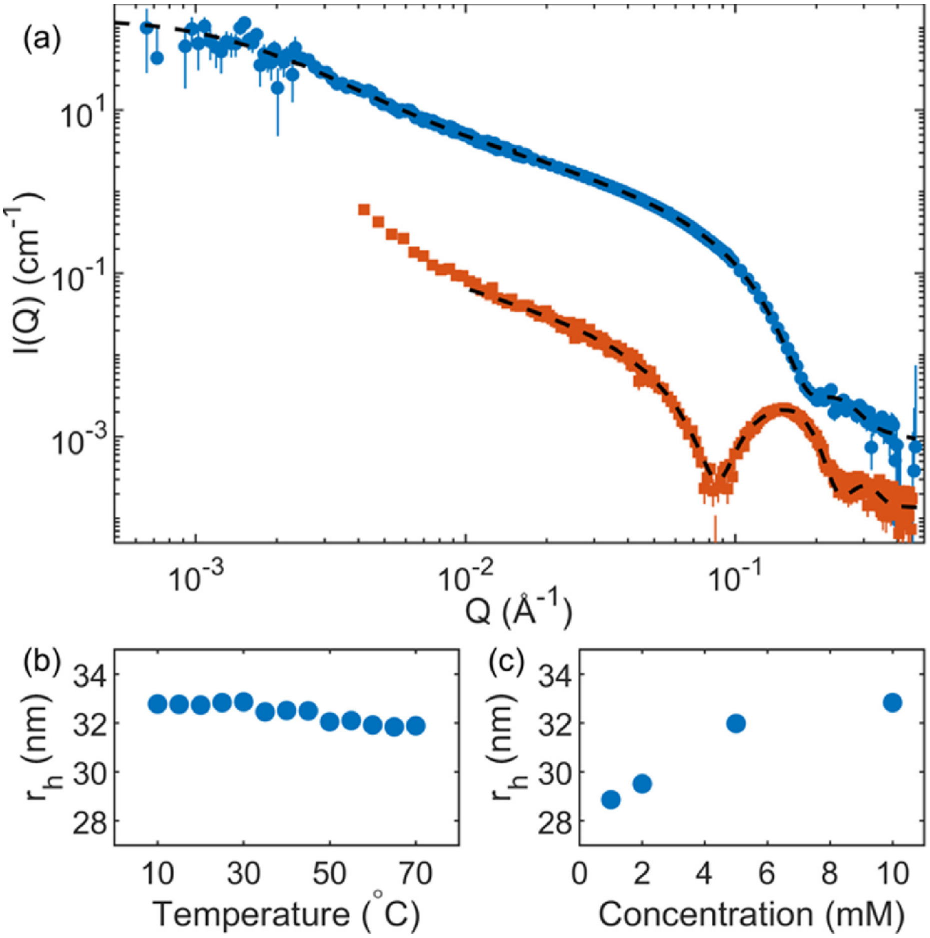

**Fig. 3.** (a) SAXS (■) and SANS (●) data and best fits of 10 mM β-$C_{16\text{-}1}G_2$ at 50 °C in $H_2O$ and $D_2O$, respectively. The black dashed lines represent the fits using the core–shell ellipsoid to the SAXS data and flexible cylinder model to the SANS data. Hydrodynamic radius ($r_h$) for 10 mM β-$C_{16\text{-}1}G_2$ in $H_2O$ (b) at different temperatures and (c) for different concentrations of β-$C_{16\text{-}1}G_2$ at 25 °C. Where not visible, error bars are within the marker size.

hardly affected by temperature changes (Fig. 3b), but there is a slight increase in micellar size with increasing concentration (Fig. 3c), potentially associated with a change in the contour length [14]. Furthermore, the headgroup solvation, i.e. the volume fraction of solvent in the headgroup region, was calculated from the fitted scattering length density of the headgroup region (X-ray SLD: 10.6 ± 0.1 × $10^{-6}$ Å$^{-2}$) and resulted in a value of 0.73 ± 0.03.

Interestingly, the contour length of the β-$C_{16\text{-}1}G_2$ micelles was found, within the experimental error, to be the same as that of the β-$C_{16}G_2$ micelles (8600 ± 200 Å). The micelle cross-section was found to be slightly smaller in the case of the unsaturated surfactant compared to that of the saturated analogue (15.5 ± 0.1 Å core radius and 16.2 ± 0.1 Å shell thickness) [15]. The differences in the cross-section are potentially attributed to changes in the conformational entropy of the tail domain (i.e. monomer packing) between the unsaturated and saturated surfactants, as observed for lipid bilayers [21]. These structural similarities are consistent with both surfactants having a similar rheological behaviour, such as the same relaxation time. The main structural difference is observed in the micelle flexibility, where the persistence length of the β-$C_{16\text{-}1}G_2$ micelles is significantly shorter than that of the β-$C_{16}G_2$ micelles (316 ± 10 Å) [15]. This difference may be attributed to the difference in the cross-sectional size of the micelles, where a thicker micelle requires more energy to bend and thus promotes a longer persistence length due to geometrical constraints [22].

## 3. Conclusions

The synthesis and behaviour of the first unsaturated sugar-based surfactant in aqueous solution are reported. The preparation of a maltoside surfactant with a $C_{16}$ monounsaturated tail (9Z) prompted a significant reduction of the Krafft point compared to the saturated counterpart [14]. Unlike other non-ionic surfactant systems [23], the solutions of β-$C_{16\text{-}1}G_2$ are not affected by clouding at high temperatures. This allowed the palmitoleyl surfactant to remain soluble from just above 0 °C up to almost 100 °C. Solutions of this surfactant show a marked non-Newtonian character, as the micellar phase leads to the formation of a viscoelastic fluid of Maxwellian character. This behaviour mimics that of the saturated surfactant at similar concentrations, with the exception of the apparent stringiness quantified by the tensile strength texture analysis [15]. Structural analysis of the micelles using a combination of scattering techniques revealed the formation of worm-like micelles, which are present in a wide range of concentrations and temperatures. The dimensions of the palmitoleyl micelles were found to be similar to those of the saturated analogue [14,15]. However, the aggregates of the palmitoleyl surfactant are more flexible than those of the saturated surfactant, which could relate to the differences in the rheological behaviour.

The greatest advantage of the preparation of sugar-based surfactants with unsaturated long tails is that it facilitates the preparation of viscosity modifiers that remain soluble in a wide temperature range, i.e. from the freezing point to the boiling point of water. This work contributes to the elaboration of a library of amphiphiles with potential applications in a variety of technologies, e.g. formulation technology and stimuli-responsive materials, with the advantage of presenting relatively simple synthetic procedure and sustainable character [11,12]. Furthermore, these results expand the possibilities of developing sugar-based surfactants where the micro- and macroscopic behaviour of the system is finely tuned through changes in the molecular structure of the surfactant, e.g. changes in the anomeric configuration and degree of tail saturation, with minimal or no change in the chemical composition of the system [14,15,24,25].

## 4. Experimental section

Palmitoleyl-β-D-maltoside ((*Z*)-Hexadec-9-en-1-yl-β-D-maltoside, β-$C_{16\text{-}1}G_2$) was synthesized and characterised ($^1$H, $^{13}$C NMR spectroscopy, and mass spectrometry) at the Deuteration and Macromolecular Crystallisation DEMAX platform (ESS, Sweden). β-$C_{16\text{-}1}G_2$ was synthesised according to literature procedures for the *n*-dodecyl analogue [26], via a Koenigs-Knorr glycosylation reaction between 2,3,6,2′,3′,4′,6′-hepta-O-acetyl-α-D-maltosyl bromide and palmitoleyl alcohol, followed by hydrolysis of the acetyl groups. Palmitoleyl alcohol was produced from palmitoleic acid, using the standard reducing reagent lithium aluminium hydride. *n*-Hexadecyl-β-D-maltoside (β-$C_{16}G_2$) was purchased from Anatrace Inc. Water of Milli-Q purity and $D_2O$ (Sigma Aldrich, 99.9% D) were used in the experiments presented here.

DSC measurements were performed on a MicroCal VP-DSC instrument using a scan rate of 30 °C/h between 5 °C and 95 °C, and water as the reference. Linear and oscillatory rheology was performed on an Anton Paar MCR 301 at 25 °C using a cone-plate geometry with a cone diameter of 25 mm, a cone angle of 1° and a gap of 0.048 mm. The flow curves were recorded in a shear rate range between 0.01 and 100 $s^{-1}$ with 7 measurements per decade. The linear viscoelastic region (LVER) was determined (see ESI), and subsequent experiments were conducted at a constant strain of 10% over the angular frequency range of 0.05–100 rad/s. Tensile strength texture analysis was conducted using a TA.XT2i instrument, Stable Micro Systems, with a hemispherical cylinder probe with a diameter of 6 mm. The applied force on the probe was 1 g and the trigger force was 1 g which submerged the probe in the sample. After 60 s the probe was lifted from the solution with a speed of 1 mm/s and the force required was recorded.

The hydrodynamic radius of the micelles ($r_h$) was determined using a Zetasizer Nano-ZS, Malvern Instruments Ltd. Measurements were performed at temperatures between 70 °C and 10 °C, with 5 °C steps. Samples were equilibrated for 5 min at each temperature and triplicates were measured for each data point. Correlation functions showed a single exponential decay and, thus, data were analysed using the cumulants method.

SAXS experiments were performed on a SAXSlab Ganesha pinhole instrument, JJ X-ray System Aps, equipped with a Xenocs X-ray microsource and a two-dimensional 300 k Pilatus detector, Dectris Ltd. Images were collected at two given sample-to-detector distances using a wavelength of $\lambda = 1.54$ Å. The configurations gave a combined momentum transfer (Q) range of 0.004–0.75 Å$^{-1}$. The azimuthally averaged intensities (I(Q)) were subtracted for the contribution of the solvent and sample stage and put to absolute scale by calibration against water.

SANS experiments were performed at the Heinz Maier-Leibnitz Zentrum, (MLZ) on the KWS-3 and KWS-2 instrument (Garching, Germany) [27,28]. On KWS-3 the wavelength of the neutrons was 12.8 Å, and two different sample-to-detector distances were used, 1.15 and 9.15 m. On KWS-2 three detector distances were used (2, 8 and 20 m) and the wavelength of the neutrons was 5 Å for 2 and 8 m and 10 Å for 20 m. The samples were loaded in quartz cuvettes with a 2-mm path length and measured at 50 °C. The raw data were reduced according to the protocol of each beamline and solvent contribution was subtracted to obtain the output files in (I(Q), in absolute intensity, vs. Q. Data from the two instruments were merged, yielding a combined Q range of 0.000183–0.0187 Å$^{-1}$.

Simultaneous analysis of the SAXS and SANS data was performed in SasView 4.2.2 by fitting to flexible cylinder and core–shell cylinder form factor models [29–31], conforming to the micellar shape, as previously reported for WLM of sugar-based surfactants [14].

For further details on the surfactant synthesis, experimental considerations and data analysis refer to the ESI.

## CRediT authorship contribution statement

**Johan Larsson:** Methodology, Investigation, Formal analysis, Writing - original draft, Writing - review & editing, Visualization. **Anna E. Leung:** Investigation, Resources, Writing - review & editing. **Christian Lang:** Investigation, Resources, Writing - review & editing. **Baohu Wu:** Investigation, Resources. **Marie Wahlgren:** Methodology, Investigation, Writing - review & editing, Funding acquisition. **Tommy Nylander:** Investigation, Writing - review & editing, Funding acquisition. **Stefan Ulvenlund:** Investigation, Writing - review & editing, Funding acquisition. **Adrian Sanchez-Fernandez:** Conceptualization, Methodology, Investigation, Formal analysis, Writing - original draft, Writing - review & editing.

## Declaration of Competing Interest

The authors declare that they have no known competing financial interests or personal relationships that could have appeared to influence the work reported in this paper.

## Acknowledgements

The Authors would like to thank the Swedish Research Council Formas (Grant 2015-666) for funding J.L. The research was also performed with financial support from Vinnova - Swedish Governmental Agency for Innovation Systems within the NextBioForm Competence Centre. This project has received funding from the European Union's Horizon 2020 research and innovation programme under grant agreement No 731019 (EUSMI). This work is based upon experiments performed on the KWS-2 and KWS-3 instruments, operated by JCNS at the Heinz Maier-Leibnitz Zentrum (MLZ), Garching, Germany (Proposal No. 16341 and 15556). This work benefited from the use of the SasView application, originally developed under NSF award DMR-0520547. SasView contains code developed with funding from the European Union's Horizon 2020 research and innovation programme under the SINE2020 project, grant agreement No 654000.

## Appendix A. Supplementary material

Supplementary data to this article can be found online at https://doi.org/10.1016/j.jcis.2020.11.063.

## References

[1] J.N. Israelachvili, D.J. Mitchell, B.W. Ninham, Theory of self-assembly of hydrocarbon amphiphiles into micelles and bilayers, J. Chem. Soc., Faraday Trans. 2 (72) (1976) 1525.

[2] M.E. Cates, S.J. Candau, Statics and dynamics of worm-like surfactant micelles, J. Phys.: Condens. Matter 2 (33) (1990) 6869–6892.

[3] G. Porte, J. Appell, Y. Poggi, Experimental investigations on the flexibility of elongated cetylpyridinium bromide micelles, J. Phys. Chem. 84 (23) (1980) 3105–3110.

[4] L.J. Magid, Z. Li, P.D. Butler, Flexibility of elongated sodium dodecyl sulfate micelles in aqueous sodium chloride: a small-angle neutron scattering study, Langmuir 16 (26) (2000) 10028–10036.

[5] J. Yang, Viscoelastic wormlike micelles and their applications, Curr. Opin. Colloid Interface Sci. 7 (5) (2002) 276–281.

[6] Z. Chu, C.A. Dreiss, Y. Feng, Smart wormlike micelles, Chem. Soc. Rev. 42 (17) (2013) 7174–7203.

[7] C.A. Dreiss, Wormlike micelles: where do we stand? Recent developments, linear rheology and scattering techniques, Soft Matter 3 (8) (2007) 956–970.

[8] C. Tanford, The Hydrophobic Effect: Formation of Micelles and Biological Membranes, John Wiley & Sons Inc, New York, 1980.

[9] S.R. Raghavan, E.W. Kaler, Highly viscoelastic wormlike micellar solutions formed by cationic surfactants with long unsaturated tails, Langmuir 17 (2) (2001) 300–306.

[10] V.T. Kelleppan, J.E. Moore, T.M. McCoy, A.V. Sokolova, L.D. Campo, B.L. Wilkinson, R.F. Tabor, Self-assembly of long-chain betaine surfactants: effect of tailgroup structure on wormlike micelle formation, Langmuir 34 (3) (2018) 970–977.

[11] J.E. Moore, T.M. McCoy, L. de Campo, A.V. Sokolova, C.J. Garvey, G. Pearson, B.L. Wilkinson, R.F. Tabor, Wormlike micelle formation of novel alkyl-tri(ethylene glycol)-glucoside carbohydrate surfactants: structure–function relationships and rheology, J. Colloid Interface Sci. 529 (2018) 464–475.

[12] J.E. Moore, T.M. McCoy, A.V. Sokolova, L. de Campo, G.R. Pearson, B.L. Wilkinson, R.F. Tabor, Worm-like micelles and vesicles formed by alkyl-oligo (ethylene glycol)-glycoside carbohydrate surfactants: the effect of precisely tuned amphiphilicity on aggregate packing, J. Colloid Interface Sci. 547 (2019) 275–290.

[13] W. von Rybinski, K. Hill, Alkyl polyglycosides—properties and applications of a new class of surfactants, Angew. Chem. Int. Ed. 37 (10) (1998) 1328–1345.

[14] J. Larsson, A. Sanchez-Fernandez, N. Mahmoudi, L.C. Barnsley, M. Wahlgren, T. Nylander, S. Ulvenlund, Effect of the anomeric configuration on the micellization of hexadecylmaltoside surfactants, Langmuir 35 (43) (2019) 13904–13914.

[15] J. Larsson, A. Sanchez-Fernandez, A.E. Leung, R. Schweins, B. Wu, T. Nylander, S. Ulvenlund, M. Wahlgren, Molecular structure of maltoside surfactants controls micelle formation and rheological behavior, J. Colloid Interface Sci. 581 (2021) 895–904.

[16] M.E. Cates, Reptation of living polymers: dynamics of entangled polymers in the presence of reversible chain-scission reactions, Macromolecules 20 (9) (1987) 2289–2296.

[17] J.F. Berret, J. Appell, G. Porte, Linear rheology of entangled wormlike micelles, Langmuir 9 (11) (1993) 2851–2854.

[18] M.E. Cates, Dynamics of living polymers and flexible surfactant micelles : scaling laws for dilution, J. Phys. France 49 (9) (1988) 1593–1600.

[19] D. Sachsenheimer, C. Oelschlaeger, S. Müller, J. Küstner, S. Bindgen, N. Willenbacher, Elongational deformation of wormlike micellar solutions, J. Rheol. 58 (6) (2014) 2017–2042.

[20] B.F. García, S. Saraji, A new insight into the dependence of relaxation time on frequency in viscoelastic surfactant solutions: from experimental to modeling study, J. Colloid Interface Sci. 517 (2018) 265–277.

[21] M. Deleu, M. Paquot, T. Nylander, Effect of fengycin, a lipopeptide produced by bacillus subtilis, on model biomembranes, Biophys. J. 94 (7) (2008) 2667–2679.

[22] J. Appell, G. Porte, Y. Poggi, Quantitative estimate of the orientational persistence length of flexible elongated micelles of cetylpyridinium bromide, J. Colloid Interface Sci. 87 (2) (1982) 492–499.

[23] P.O. Cummins, J.B. Hayter, J. Penfold, E. Staples, A small-angle neutron scattering investigation of shear-aligned hexaethyleneglycolmonohexadecylether (C16E6) micelles as a function of temperature, Chem. Phys. Lett. 138 (5) (1987) 436–440.

[24] C.A. Ericsson, O. Söderman, S. Ulvenlund, Aggregate morphology and flow behaviour of micellar alkylglycoside solutions, Colloid. Polym. Sci. 283 (12) (2005) 1313–1320.

[25] F. Nilsson, O. Söderman, I. Johansson, Four different C8G1Alkylglucosides. anomeric effects and the influence of straight vs branched hydrocarbon chains, J. Colloid Interface Sci. 203 (1) (1998) 131–139.

[26] S.R. Midtgaard, T.A. Darwish, M.C. Pedersen, P. Huda, A.H. Larsen, G.V. Jensen, S.A.R. Kynde, N. Skar-Gislinge, A.J.Z. Nielsen, C. Olesen, M. Blaise, J.J. Dorosz, T. S. Thorsen, R. Venskutonytė, C. Krintel, J.V. Møller, H. Frielinghaus, E.P. Gilbert, A. Martel, J.S. Kastrup, P.E. Jensen, P. Nissen, L. Arleth, Invisible detergents for structure determination of membrane proteins by small-angle neutron scattering, The FEBS J. 285 (2) (2018) 357–371.

[27] V. Pipich, Z. Fu, KWS-3: Very small angle scattering diffractometer with focusing mirror, J. Large-scale Res. Facilities JLSRF 1 (2015) 31.

[28] A. Radulescu, N.K. Székely, M.-S. Appavou, KWS-2: Small angle scattering diffractometer, J. Large-scale Res. Facilities JLSRF 1 (2015).

[29] J.S. Pedersen, Analysis of small-angle scattering data from colloids and polymer solutions: modeling and least-squares fitting, Adv. Colloid Interface Sci. 70 (1997) 171–210.

[30] J.S. Pedersen, P. Schurtenberger, Scattering functions of semiflexible polymers with and without excluded volume effects, Macromolecules 29 (23) (1996) 7602–7612.

[31] M.C. Doucet, Jae Hie, Alina, Gervaise, Bakker, Jurrian, Bouwman, Wim, Butler, Paul, Campbell, Kieran, Gonzales, Miguel, Heenan, Richard, Jackson, Andrew, Juhas, Pavol, King, Stephen, Kienzle, Paul, Krzywon, Jeff, Markvardsen, Anders, Nielsen, Torben, O'Driscoll, Lewis, Potrzebowski, Wojciech, Ferraz Leal, Ricardo, Richter, Tobias, Rozycko, Piotr, Snow, Tim, Washington, Adam, SasView version 4.2.2, 2019. https://doi.org/10.5281/zenodo.2652478.